International Journal of Advances in Engineering and Management (IJAEM)
Volume 4, Issue 9 Sep. 2022, pp: 733-740 www.ijaem.net ISSN: 2395-5252

Performance Analysis of Three-Phase Solar PV Integrated UPQC

Bhumika Akade[1], Dr. V. M. Jape[2]
[1]*Bhumika Akade, Mtech Student, GCOE, Amravati.*
[2]*Dr. V. M. Jape, Dept. of Electrical engineering GCOE, Amravati, Maharashtra, India.*

Date of Submission: 07-09-2022 Date of Acceptance: 17-09-2022

ABSTRACT— The design and performance evaluation of a three-phase single stage solar photovoltaic integrated unified power quality conditioner are the topics of this article (PV-UPQC). Shunt and series voltage compensators are coupled back to back with a shared DC-link to form the PV-UPQC. Along with adjusting for load current harmonics, the shunt compensator also extracts energy from a PV array. The PVUPQC performs better thanks to an improved synchronous reference frame control based on a moving average filter that extracts the load active current component. Grid voltage sags and swells are just two examples of the power quality issues that the series compensator corrects. During sag and swell circumstances, the compensator injects voltage that is either in phase or out of phase with the point of common coupling (PCC) voltage. The system being suggested combines both the advantages of producing clean energy and raising the standard of power. Through simulation in Matlab-Simulink with a nonlinear load, the system's steady state and dynamic performance are assessed.

Key Words: Power Quality, shunt compensator, series compensator, UPQC, Solar PV, MPPT

I. INTRODUCTION

The penetration of power electronic loads has expanded with the development of semiconductor technology. The efficiency of these loads, which include computer power supplies, variable speed drives, switched mode power supplies, etc., is quite high, yet they require nonlinear currents. Particularly in distribution systems, these nonlinear currents result in voltage distortion at the point of common coupling. Additionally, there is a growing focus on the production of clean energy through the installation of rooftop PV systems in both commercial buildings and small dwellings [1], [2]. However, because PV energy sources are sporadic in nature, more of these systems being installed, especially in underdeveloped distribution networks, causes voltage quality issues including voltage sags and swells, which ultimately lead to grid instability [3]–[7].

These voltage quality issues also cause power electronic systems to frequently trip falsely, electronic systems to malfunction and trip falsely, and capacitor banks to heat up more quickly, among other things. [8]–[10]. Modern distribution systems struggle with significant power quality concerns on both the load side and the grid side. Multifunctional systems that can integrate clean energy generation and power quality enhancement are required due to the demand for clean energy as well as the strict power quality requirements of advanced electronic loads. In [11], [12], a three-phase, multi-functional solar energy conversion system that corrects load side power quality issues was proposed. In [13], [14], a single phase solar pv inverter with active power filtering capability has been suggested Shunt active filtering and clean energy generation have been the subject of extensive investigation. Shunt active filtering is capable of regulating the load voltage as well, but it also introduces reactive power. As a result, shunt active filtering is unable to simultaneously maintain grid current unity power factor and PCC voltage regulation. Recently, the usage of series active filters has been suggested for use in small residences and commercial buildings due to the strict voltage quality requirements for sophisticated electronics loads [15], [16]. In [17], A dynamic voltage restorer and a solar photovoltaic system were integrated. In contrast to shunt and series active power filters, a unified power quality conditioner (UPQC), which includes both shunt and series compensators, may regulate load voltage and keep grid current sinusoidal at unity power factor simultaneously. The integration of a PV array and UPQC provides both clean energy generation and universal active. The integration of UPQC and a PV array has been documented in [18] through [20]. The solar PV integrated UPQC has many advantages over traditional grid-connected inverters, including increased fault ride through capabilities of the

International Journal of Advances in Engineering and Management (IJAEM)
Volume 4, Issue 9 Sep. 2022, pp: 733-740 www.ijaem.net ISSN: 2395-5252

converter during transients, protection of key loads from grid side disturbances, and improved power quality of the grid. There is a resurgence of interest in UPQC systems due to the increased focus on distributed generation and microgrids [21], [22].

The creation of reference signals is a crucial component of PV-UPQC control. The two primary categories of reference signal generating techniques are time-domain and frequency domain procedures [8]. Because real-time implementation requires less computing, time domain techniques are frequently used. Instantaneous reactive power theory (p-q theory), synchronous reference frame theory (d-q theory), and instantaneous symmetrical component theory are some of the often employed methods [23]. The fundamental problem with using synchronous reference frame theory-based methods is that they produce double harmonic components in the d-axis current when the load is imbalanced. This calls for the employment of low pass filters with extremely low cutoff frequencies to filter out dual harmonic element Poor dynamic performance follows from this [24]. In this study, the fundamental load active current is obtained by filtering the d-axis current using a moving average filter (MAF). This provides the best attenuation while not affecting the controller's bandwidth [25]. Recently, MAF has been used to synchronize the grid utilizing phase locked loops and improve the performance of DC-link controllers (PLL).

The design and performance analysis of a three phase PV-UPQC are provided in this research. The dynamic performance during load active current extraction is enhanced by a MAF-based d-q theory-based control. The following are the system's primary benefits:

• Integration of the production of clean energy and the enhancement of electricity quality.
• A simultaneous improvement in voltage and current quality.
• Better load current adjustment as a result of MAF use in PV-d-q UPQC's control.
• Stable under a range of dynamic circumstances, including voltage sags/swells, load imbalance, and irradiation variation.

Using Matlab-Simulink software, the suggested system's performance is thoroughly examined in both dynamic and steady state circumstances.

II. SYSTEM CONFIGURATION AND DESIGN

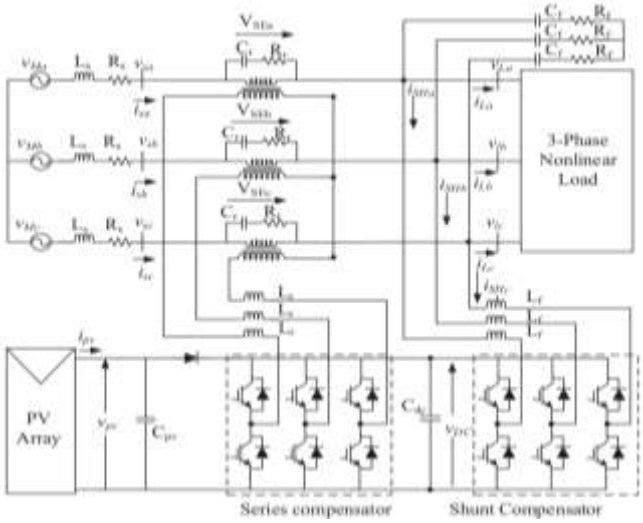

Fig. 1. System Configuration PV-UPQC

Fig. 1 depicts the PV-structural UPQC's layout. The three-phase system is intended for by the PV-UPQC. Shunt and series compensators are coupled by a common DC-bus to form the PV-UPQC. The load side is where the shunt compensator is linked.

Through a reverse blocking diode, the solar PV array is directly connected to the DC-link of the UPQC. The series compensator corrects for grid voltage sags and swells while operating in voltage management mode. Through interface inductors, the grid is interconnected with the shunt and series compensators.

Voltage produced by the series compensator is fed into the grid via a series injection transformer. Harmonics produced by converter switching are filtered using ripple filters. The applied load is a nonlinear load made up of the load is a voltage-fed load with a bridge rectifier, making it a nonlinear load.

International Journal of Advances in Engineering and Management (IJAEM)
Volume 4, Issue 9 Sep. 2022, pp: 733-740 www.ijaem.net ISSN: 2395-5252

2.1 Design of PV-UPQC

The appropriate sizing of the PV array, DC-link capacitor, DC-Link voltage level, etc., is the first step in the design process for PV-UPQC. In addition to compensating for the load current's reactive power and current harmonics, the shunt compensator is sized so that it can manage the peak power output from the PV array. The PV array is sized so that the MPP voltage is the same as the intended DC-link voltage because it is directly incorporated into the UPQC DC-link. The rating is set up so that, in ideal circumstances, the PV array sends both power to the grid and the active power required by the load. In Appendix A, the particular PV array specifications are listed. The series injection transformer of the series compensator and the interacting inductors of the shunt and series compensators are the other planned components. The PV-UPQC design is described in the sections below.

1.**Voltage Magnitude of DC-Link**: The magnitude of DC-link voltage Vdc depends on the depth of modulation used and per-phase voltage of the system. The DC-link voltage magnitude should more than double the peak of per-phase voltage of the three phase system[8] and is given as

$$Vdc = \frac{2\sqrt{2}V_{LL}}{\sqrt{3}m} \quad (1)$$

where depth of modulation (m) is taken as 1 and VLL is the grid line voltage. For a line voltage of 415 V, the required minimum value DC-bus voltage is 677.7 V. The DC-bus voltage is set at 700 V(approx), which is same as the MPPT operating voltage of PV array at STC conditions.

2.DC-Bus Capacitor Rating: The DC-link capacitor is sized based upon power requirement as well as DC-bus voltage level. The energy balance equation for the DC-bus capacitor is given as follows [8],

$$C_{dc} = \frac{3k_a V_{ph} I_{sh}}{0.5 \times (V_{dc}^2 - V_{dc1}^2)}$$

$$C_{dc} = \frac{3 \times 0.1 \times 1.5 \times 239.6 \times 34.5 \times 0.03}{0.5 \times (700^2 - 677.79^2)}$$

$$C_{dc} = 9.3mf \quad (2)$$

where V_{dc} is the average DC-bus voltage, V_{dc1} is the lowest required value of DC-bus voltage, a is the overloading factor, V_{ph} is per-phase voltage, t is the minimum time required for attaining steady value after a disturbance, I_{sh} is per-phase current of shunt compensator, k factor considers variation in energy during dynamics. The minimum required DC-link voltage is V_{dc1} = 677.69 V as obtained from (2), V_{dc} = 700 V, V_{ph}= 239.60 V, I_{sh}=57.5 A, t= 30 ms, a = 1.2, and for dynamic energy change = 10%, k= 0.1, the value of C_{dc} is obtained as 9.3 mf.

where V_{LL} is the grid line voltage and depth of modulation (m) is assumed to be 1. The required minimum DC-bus voltage for a 415 V line is 677.7 V, and the DC-bus voltage is set at 700 V (approximately), which is the same as the MPPT operating voltage of a PV array under STC conditions.

2.DC-Bus Capacitor Rating: The power needs and DC-bus voltage level are used to size the DC-link capacitor. The following is the energy balance equation for the DC-bus capacitor [8],

$$L_f = \frac{\sqrt{3}mV_{dc}}{12af_{sh}I_{cr,pp}} = \frac{\sqrt{3} \times 1 \times 700}{12 \times 1.2 \times 10000 \times 6.9}$$

$$= 800\mu H \approx 1mH \quad (3)$$

where V_{dc} is the average DC-bus voltage, V_{dc1} is the minimum required DC-bus voltage, an is the overloading factor, V_{ph} is the per-phase voltage, t is the shortest time necessary to reach steady state after a disturbance, and I_{sh} is the per-phase current of the shunt compensator, and the k factor takes energy variation during dynamics into account. According to (2), the minimum necessary DC-link voltage is V_{dc1} = 677.69 V, V_{dc} = 700 V, V_{ph} = 239.60 V, I_{sh} = 57.5 A, t = 30 ms, a = 1.2, and the value of C_{dc} is 9.3 mf for a dynamic energy shift of 10%, k = 0.1

3) Interfacing Inductor of Shunt Compensator: The interfacing inductor rating of the shunt compensator depends upon the ripple current, the switching frequency and DC-link voltage. The expression for the interfacing inductor is as

$$L_f = \frac{\sqrt{3}mV_{dc}}{12af_{sh}I_{cr,pp}} = \frac{\sqrt{3} \times 1 \times 700}{12 \times 1.2 \times 10000 \times 6.9}$$

$$= 800\mu H \approx 1mH \quad (3)$$

where m is depth of modulation, a is pu value of maximum overload, f_{sh} is the switching frequency , $I_{cr,pp}$ is the inductor ripple current which is taken as 20% of rms phase current of shunt compensator. Here, m=1, a=1.2, f_{sh}=10kHz, V_{dc}=700V, one gets 800 µH as value. The value chosen is approximated to 1mH.

4) Series Injection Transformer: The PV-UPQC is designed to compensate for a sag/swell of 0.3 pu i.e 71.88 V. Hence, the required voltage to be injection is only 71.88 V which results in low modulation index for the series compensator when the DC-link voltage is 700V. In order to operate the series compensator with minimum harmonics, one keeps modulation index of the series compensator near to unity. Hence a series transformer is used with a turns ratio,

$$K_{SE} = \frac{V_{VSC}}{V_{SE}} = 3.33 \approx 3 \quad (4)$$

The value obtained for K_{SE} is 3.33. The value selected is 3. The rating of series injection transformer is given as,

International Journal of Advances in Engineering and Management (IJAEM)
Volume 4, Issue 9 Sep. 2022, pp: 733-740 www.ijaem.net ISSN: 2395-5252

$$S_{SE} = 3V_{SE}I_{SE_{sag}} = 3 \times 72 \times 46 = 10kVA \quad (5)$$

The current through series VSC is same as grid current. The supply current under sag condition of 0.3 pu is 46 A and hence the VA rating of injection transformer achieved is 10 kVA.

5) Interfacing Inductor of Series Compensator: The rating of interfacing inductor of the series compensator depends on ripple current at swell condition, switching frequency and DC link voltage. Its value is expressed as,

$$L_r = \frac{\sqrt{3} \times mV_{dc}K_{SE}}{12af_{se}I_r} = \frac{\sqrt{3} \times 1 \times 700 \times 3}{12 \times 1.2 \times 10000 \times 7.1} = 3.6mH \quad (6)$$

where m is the depth of modulation, a is the pu value of maximum overload, f_{se} is the switching frequency, I_r is the inductor current ripple, which is taken to be 20% of grid current. Here, m=1, a=1.5, f_{se}=10 kHz, V_{dc}=700 V and 20% ripple current, one gets 3.6 mH as selected value.

III. CONTROL OF PV-UPQC

Shunt compensator and series compensator are two of PV-primary UPQC's subsystems. Problems with load power quality, like load current harmonics and load reactive power, are corrected by the shunt compensator. The shunt compensator in a PV-UPQC system also supplies power from the solar PV array. Utilizing the maximum power point tracking (MPPT) algorithm, the shunt compensator draws power from the PV array. By injecting the proper voltage in phase with the grid voltage, the series compensator shields the load from grid side power quality issues such voltage sags and swells.

A. Management of the Shunt Compensator

By running the solar PV array at its highest power setting, the shunt compensator gets the most power out of it. Powerpoint tracking at its maximum (MPPT) The reference voltage for the PV-DC-link UPQC's is produced using an algorithm. Perturb and Observe (P& O) algorithm and incremental conductance algorithm are two examples of popular MPPT algorithms [28]. (INC).

In this work, MPPT is implemented using the (P&O) algorithm. A PI-controller is used to keep the DC-link voltage at the generated reference. The shunt compensator extracts the active fundamental component of the load current to carry out the load current compensation. In this work, the fundamental active component of the load current is extracted using the SRF technique to operate the shunt compensator.

In Fig.2, the shunt compensator's control structure is depicted. 2. The phase and frequency data collected by PLL is used to convert the load currents to the d-q-0 domain. PCC voltage is the PLL input. The fundamental component in the abc frame of reference is extracted from the load current's d-component (ILd) by filtering out the DC component (ILdf). A moving average filter (MAF) is used to extract the DC component so that the dynamic performance is not negatively impacted. As follows is the moving average filter's transfer function:

$$MAF(s) = \frac{1 - e^{-T_w s}}{T_w s} \quad (7)$$

where the moving average filter's window length (T_w) is concerned. Tw is preserved at half of the highest harmonic because the lowest harmonic in the d-axis current is a double harmonic component, Tw is maintained at 50% of the fundamental time period. The MAF has integer multiples of zero gain and unity DC gain. The corresponding current component resulting from the PV array is provided as,

$$I_{pvg} = \frac{2}{3}\frac{P_{pv}}{V_s} \quad (8)$$

where Vs is the size of the PCC voltage and Ppv is the power of the PV array. Reference grid current is represented as

$$I^*_{sd} = I_{Ldf} + I_{loss} - I_{pvg} \quad (9)$$

I^*_{sd} is transformed into grid currents for the abc domain. In a hysteresis current controller, the measured and reference grid currents are compared to produce the gating pulses for the shunt converter.

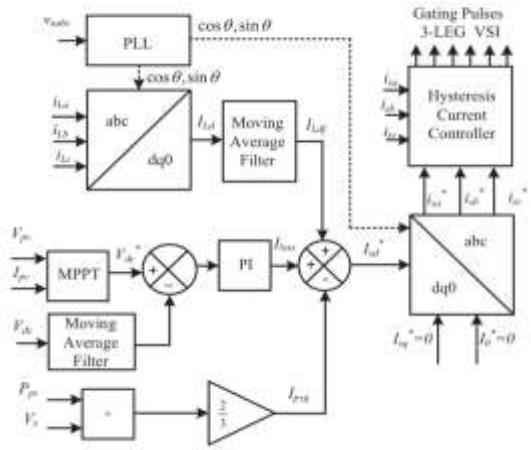

Fig. 2. Control Structure of Shunt Compensator

B. Control of Series Compensator

Pre-sag compensation, in-phase compensation, and energy optimal compensation are the three control strategies for the series compensator. The series compensator in this study injects voltage in

International Journal of Advances in Engineering and Management (IJAEM)
Volume 4, Issue 9 Sep. 2022, pp: 733-740 www.ijaem.net ISSN: 2395-5252

the same phase as the grid voltage, resulting in the series compensator injecting the least amount of voltage possible. Various compensation algorithms utilised for controlling the series compensator are described in detail in [29], [30].

Figure 3 depicts the control architecture of the series compensator. Using a PLL to generate the reference axis in the d q-0 domain, the fundamental component of PCC voltage is extracted. The phase and frequency data of the PCC voltage collected via PLL is used to generate the reference load voltage. The voltages from the PCC and the load are transformed into the d-q-0 domain. The peak load reference voltage is the value of the d-axis component of the load reference voltage since the reference load voltage needs to be in phase with the PCC voltage.

Keep the q-axis component at zero. The reference voltage for the series compensator is determined by the difference between the load reference voltage and PCC voltage. The real series compensator voltages are determined by the difference between the load voltage and PCC voltage. To produce the proper reference signals, PI controllers receive the difference between the reference and actual series compensator voltages.

To provide suitable gating signals for the series compensator, these signals are translated to abc domain and fed via a pulse width modulation (PWM) voltage controller.

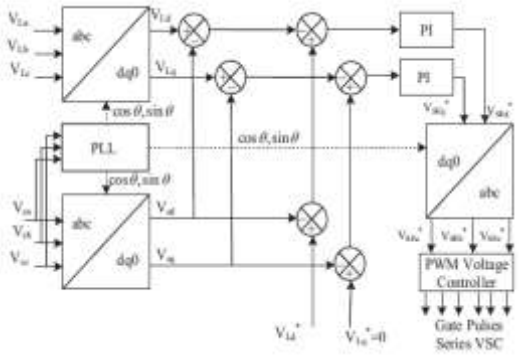

Fig. 3. Control Structure of Series Compensator

IV. SIMULATION STUDIES

By simulating the system in Matlab-Simulink software, the steady state and dynamic performances of PV-UPQC are examined. Three phase diode bridge rectifier with R-L load is the nonlinear load being employed. The simulation uses a solver step size of 1e-6s. The system is exposed to a variety of dynamic situations, including changes in PV irradiance and PCC voltage that sag and swell. The appendix contains a list of the specific system settings.

A. Performance of PV-UPQC at PCC Voltage Fluctuations

Fig. 4 displays the PV-dynamic UPQC's performance when PCC voltage sags or swells. The illumination(G) is maintained at 1000W/m2. The numerous detected signals include grid currents (i_S), load currents (i_{La}, i_{Lb}, i_{Lc}), series compensator currents (i_S), PCC voltages (v_s), load voltages (V_L), series compensator voltages (V_{SE}), DC-link voltage (V_{dc}), solar PV array current (I_{pv}), and solar PV array power (P_{pv}) (i_{SHa}, i_{SHb}, i_{SHc}). There is a voltage sag of 0.3pu between 0.7 and 0.75 seconds and a voltage swell of 0.3pu between 0.8 and 0.85 seconds.

Under these circumstances, the series compensator maintains the load voltage at the rated voltage condition by injecting a suitable voltage VSE in the opposite phase of the grid voltage disturbance.

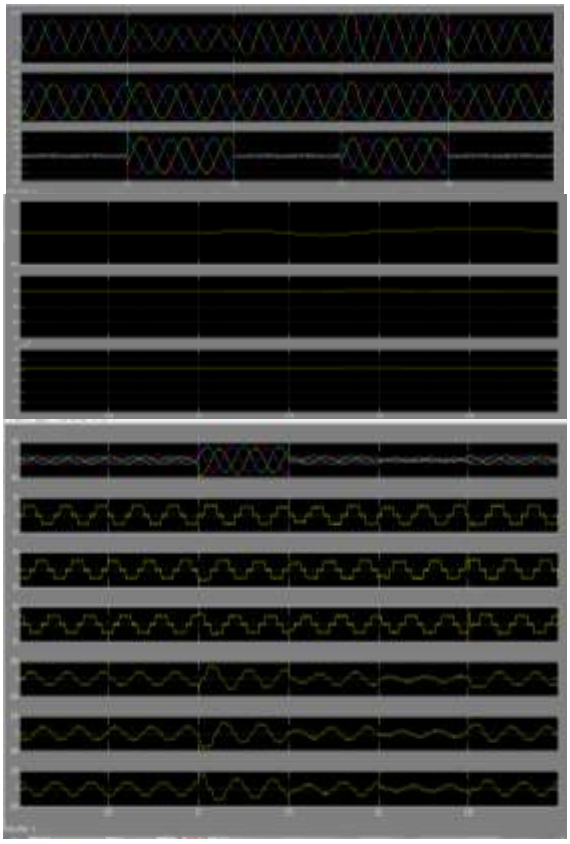

Fig. 4. Performance of PV-UPQC under Voltage Sag and Swell Conditions

B. Performance of PV-UPQC at Load Unbalancing Condition

Fig. 5 displays the dynamic performance of PV-UPQC under load unbalance conditions. Phase "b" of the load is disconnected at time t=0.8s. The grid current is sinusoidal and has a unity power factor, as

International Journal of Advances in Engineering and Management (IJAEM)
Volume 4, Issue 9 Sep. 2022, pp: 733-740 www.ijaem.net ISSN: 2395-5252

can be shown. Due to the decrease in total effective load, the current fed into the grid increases. In addition to being steady, the DC-link voltage is kept close to its target regulated value of 700V.

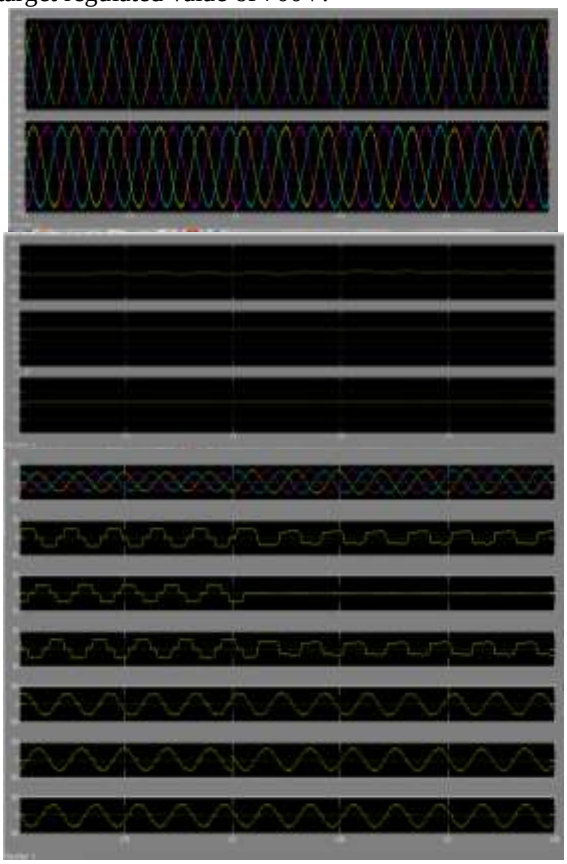

fig. 6. Performance PV-UPQC during Load Unbalance Condition

C. Performance of PV-UPQC under Varying Irradiation :The dynamic performance of PV-UPQC under varying solar irradiation is shown in Figure 6. The sun's irradiation varies from 500W/m2 at 0.8 seconds to 1000W/m2 at 0.85 seconds. It has been discovered that as irradiation increases, PV array output increases and grid current increases since the PV array is feeding power into the grid. Shunt compensators correct harmonics brought on by load current and track MPPT. The harmonic spectra, THD load current, and grid current are shown in Figures 7 and 8. In accordance with the IEEE-519 standard, the load current THD was discovered to be 26.31% and the grid current THD was detected to be 2.0%.

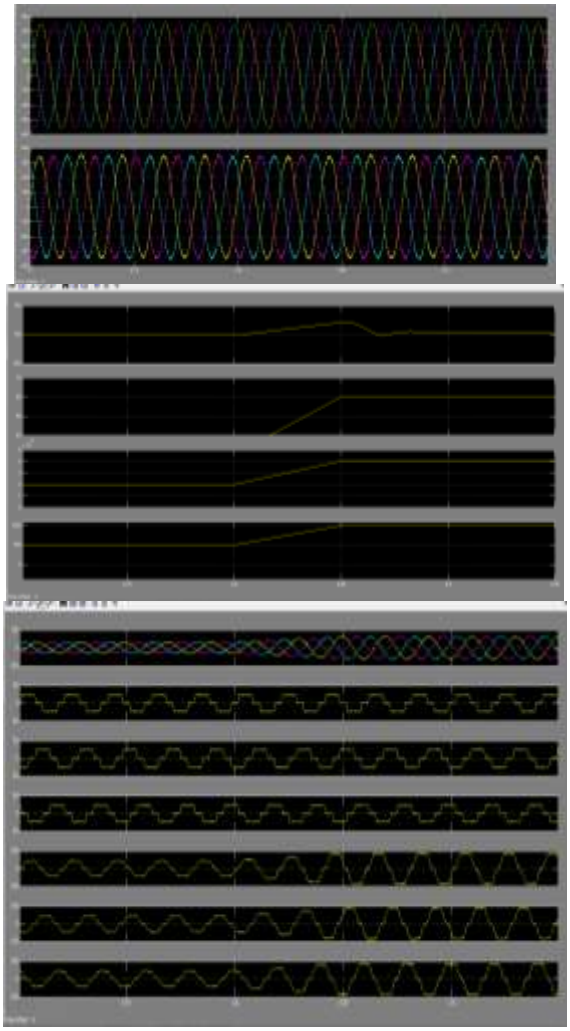

V. CONCLUSIONS

Three-phase PV-design UPQC's and dynamic performance have been examined in the context of changing irradiation and grid voltage sags/swells. Experiments on a smaller laboratory prototype have been used to validate the system's performance. It has been found that PV-UPQC reduces harmonics brought on by nonlinear loads and maintains grid current THD within the confines of the IEEE-519 standard. It is discovered that the system is stable under changing irradiation, voltage sags/swells, and load unbalance.

Specifically in load unbalanced conditions, the performance of d-q control has been enhanced by the employment of moving average filter. It can be seen that PV-UPQC, which combines distributed generation with power quality improvement, is a promising solution for contemporary distribution systems.

REFERENCES

[1]. B. Mountain and P. Szuster, “Solar, solar everywhere: Opportunities and challenges for

australia's rooftop pv systems," IEEE Power and Energy Magazine, vol. 13, no. 4, pp. 53–60, July 2015.

[2]. A. R. Malekpour, A. Pahwa, A. Malekpour, and B. Natarajan, "Hierarchical architecture for integration of rooftop pv in smart distribution systems," IEEE Transactions on Smart Grid, vol. PP, no. 99, pp. 1–1, 2017.

[3]. Y. Yang, P. Enjeti, F. Blaabjerg, and H. Wang, "Wide-scale adoption of photovoltaic energy: Grid code modifications are explored in the distribution grid," IEEE Ind. Appl. Mag., vol. 21, no. 5, pp. 21–31, Sept 2015.

[4]. M. J. E. Alam, K. M. Muttaqi, and D. Sutanto, "An approach for online assessment of rooftop solar pv impacts on low-voltage distribution networks," IEEE Transactions on Sustainable Energy, vol. 5, no. 2, pp. 663–672, April 2014.

[5]. J. Jayachandran and R. M. Sachithanandam, "Neural network-based control algorithm for DSTATCOM under nonideal source voltage and varying load conditions," Canadian Journal of Electrical and Computer Engineering, vol. 38, no. 4, pp. 307–317, Fall 2015.

[6]. A. Parchure, S. J. Tyler, M. A. Peskin, K. Rahimi, R. P. Broadwater, and M. Dilek, "Investigating pv generation induced voltage volatility for customers sharing a distribution service transformer," IEEE Trans. Ind. Appl., vol. 53, no. 1, pp. 71–79, Jan 2017.

[7]. E. Yao, P. Samadi, V. W. S. Wong, and R. Schober, "Residential demand side management under high penetration of rooftop photovoltaic units," IEEE Transactions on Smart Grid, vol. 7, no. 3, pp. 1597–1608, May 2016.

[8]. B. Singh, A. Chandra and K. A. Haddad, Power Quality: Problems and Mitigation Techniques. London: Wiley, 2015.

[9]. M. Bollen and I. Guo, Signal Processing of Power Quality Disturbances. Hoboken: Johm Wiley, 2006.

[10]. P. Jayaprakash, B. Singh, D. Kothari, A. Chandra, and K. Al-Haddad, "Control of reduced-rating dynamic voltage restorer with a battery energy storage system," IEEE Trans. Ind. Appl., vol. 50, no. 2, pp. 1295– 1303, March 2014.

[11]. B. Singh, C. Jain, and S. Goel, "ILST control algorithm of single stage dual purpose grid connected solar pv system," IEEE Trans. Power Electron., vol. 29, no. 10, pp. 5347–5357, Oct 2014.

[12]. R. K. Agarwal, I. Hussain, and B. Singh, "Three-phase single-stage grid tied solar pv ecs using PLL-less fast CTF control technique," IET Power Electronics, vol. 10, no. 2, pp. 178–188, 2017.

[13]. Y. Singh, I. Hussain, B. Singh, and S. Mishra, "Single-phase solar gridinterfaced system with active filtering using adaptive linear combiner filter-based control scheme," IET Generation, Transmission Distribution, vol. 11, no. 8, pp. 1976–1984, 2017.

[14]. T.-F. Wu, H.-S. Nien, C.-L. Shen, and T.-M. Chen, "A single-phase inverter system for pv power injection and active power filtering with nonlinear inductor consideration," IEEE Trans. Ind. Appl., vol. 41, no. 4, pp. 1075–1083, July 2005.

[15]. A. Javadi, A. Hamadi, L. Woodward, and K. Al-Haddad, "Experimental investigation on a hybrid series active power compensator to improve power quality of typical households," IEEE Trans. Ind. Electron., vol. 63, no. 8, pp. 4849–4859, Aug 2016.

[16]. A. Javadi, L. Woodward, and K. Al-Haddad, "Real-time implementation of a three-phase thseaf based on vsc and p+r controller to improve power quality of weak distribution systems," IEEE Transactions on Power Electronics, vol. PP, no. 99, pp. 1–1, 2017.

[17]. A. M. Rauf and V. Khadkikar, "Integrated photovoltaic and dynamic voltage restorer system configuration," IEEE Transactions on Sustain able Energy, vol. 6, no. 2, pp. 400–410, April 2015.

[18]. S. Devassy and B. Singh, "Design and performance analysis of three phase solar pv integrated upqc," in 2016 IEEE 6th International Con ference on Power Systems (ICPS), March 2016, pp. 1–6.

[19]. K. Palanisamy, D. Kothari, M. K. Mishra, S. Meikandashivam, and I. J. Raglend, "Effective utilization of unified power quality conditioner for interconnecting PV modules with grid using power angle control method," International Journal of Electrical Power and Energy Systems, vol. 48, pp. 131 – 138, 2013.

[20]. S. Devassy and B. Singh, "Modified p-q theory based control of solar pv integrated upqc-s," IEEE Trans. Ind. Appl., vol. PP, no. 99, pp. 1–1, 2017.

[21]. S. K. Khadem, M. Basu, and M. F. Conlon, "Intelligent islanding and seamless reconnection technique for microgrid with upqc," IEEE Journal of Emerging and Selected Topics in Power Electronics, vol. 3, no. 2, pp. 483–492, June 2015.

[22]. J. M. Guerrero, P. C. Loh, T. L. Lee, and M. Chandorkar, "Advanced control architectures for intelligent microgrids;part ii: Power quality, energy storage, and ac/dc microgrids," IEEE Transactions on Industrial Electronics, vol. 60, no. 4, pp. 1263–1270, April 2013.

[23]. B. Singh and J. Solanki, "A comparison of control algorithms for dstatcom," IEEE Transactions on Industrial Electronics, vol. 56, no. 7, pp. 2738–2745, July 2009.

[24]. B. Singh, C. Jain, S. Goel, A. Chandra, and K. Al-Haddad, "A multifunctional grid-tied solar energy conversion system with anf-based control approach," IEEE Transactions on Industry Applications, vol. 52, no. 5, pp. 3663–3672, Sept 2016.

[25]. S. Golestan, M. Ramezani, J. M. Guerrero, and M. Monfared, "dq-frame cascaded delayed signal cancellation- based pll: Analysis, design, and comparison with moving average filter-based pll," IEEE Transactions on Power Electronics, vol. 30, no. 3, pp. 1618–1632, March 2015.

[26]. R. Pea-Alzola, D. Campos-Gaona, P. F. Ksiazek, and M. Ordonez, "Dc□ link control filtering options for torque ripple reduction in low-power wind turbines," IEEE Trans. Power Electron., vol. 32, no. 6, pp. 4812–4826, June 2017.

[27]. S. Golestan, M. Ramezani, J. M. Guerrero, F. D. Freijedo, and M. Mon□ fared, "Moving average filter based phase-locked loops: Performance analysis and design guidelines," IEEE Trans. Power Electron., vol. 29, no. 6, pp. 2750–2763, June 2014.

[28]. B. Subudhi and R. Pradhan, "A comparative study on maximum power point tracking techniques for photovoltaic power systems," IEEE Trans actions on Sustainable Energy, vol. 4, no. 1, pp. 89–98, Jan 2013.

[29]. A. Sadigh and K. Smedley, "Review of voltage compensation methods in dynamic voltage restorer DVR," in IEEE Power and Energy Society General Meeting, July 2012, pp. 1–8.

[30]. A. Rauf and V. Khadkikar, "An enhanced voltage sag compensation scheme for dynamic voltage restorer," IEEE Trans. Ind. Electron., vol. 62, no. 5, pp. 2683–2692, May 2015.

[31]. "IEEE recommended practices and requirements for harmonic control in electrical power systems," IEEE Std 519-1992, pp. 1–112, April 1993.